ISBN: 978-3-95450-184-7 doi:10.18429/JACoW-IPAC2018-WEPAL020

MEASUREMENT OF TRANSVERSE DIPOLE AND QUADRUPOLE MOMENTS WITH THE BPMS IN THE J-PARC 3-50 BT

T. Toyama†, M. Tejima, H. Kuboki, K. Satou, KEK, 305-0801 Tsukuba, Ibaraki, Japan

Abstract

We measure dipole and quadrupole moments of the beam using the BPMs in the beam transport line 3-50BT of J-PARC and obtain differences of squared horizontal- and vertical-rms-sizes for those BPMs. Then we obtain rms emittances and rms momentum by fitting with given Twiss parameters.

INTRODUCTION

To measure beam sizes, or equivalently emittances in a non-destructive manner is highly required in high intensity beam accelerator facilities such as J-PARC. In the beam transport line, 3-50BT, which transfers the 3 GeV proton beam from the 3GeV Rapid Cycling Synchrotron to the 30 GeV Main Ring synchrotron (MR) (Fig.1), 14 four-parallel-plate BPMs with nonlinear position response are originally installed in contrast to the BPMs with linear position response in the MR. Making full use of this nonlinearity of 14 BPMs, we have been measuring dipole [1, 2] and quadrupole moments of the beam. Based on the method in references [3, 4, 5] we obtain root-mean-square (rms) emittances of horizontal and vertical planes and a rms momentum spread with fitting those parameters to the measured dipole and quadrupole moments with given Twiss parameters and momentum dispersion functions. The extension of the method with adding three additional four-loop-coupler BPMs [6] is under way.

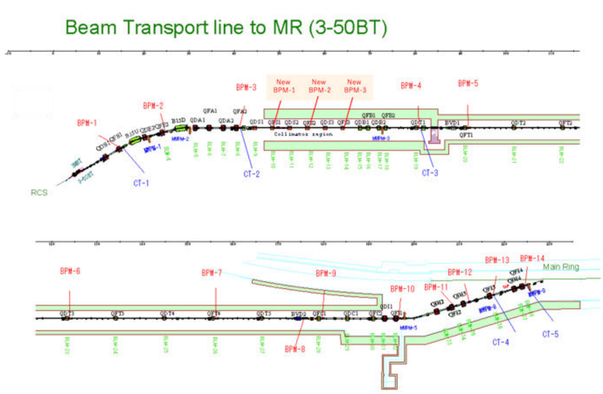

Figure 1: BPMs of the “3-50BT” beam transport line.

3-50BT BPMS

The structure of the originally installed ESM-type BPM is shown in Fig. 2. There are two kinds of geometries, a diameter of 230 mm for #1 and #2 BPMs, and 200 mm for #3 - #14 BPMs. Each BPM has four electrodes with the opening angle of 60 degree. Their locations are indicated with red characters in Fig. 1. In addition to these BPMs, three BPMs are installed at the collimator area, according to the request from the beam commissioning group [6]. The electrodes with wide opening angle would become a source of secondary electron emission due to collimated particles impinging on the surface. Therefore we chose loop type pickups with small opening angle as Fig. 3.

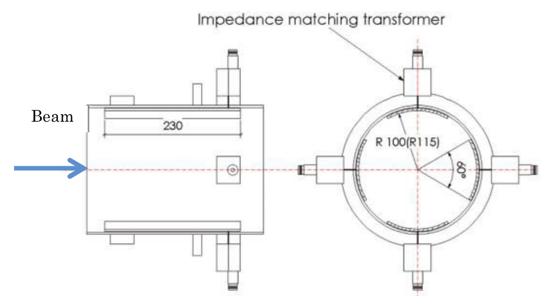

Figure 2: BPM head. There are two diameter sizes: ϕ230 (#1, 2) and ϕ200 mm (#3 - #14).

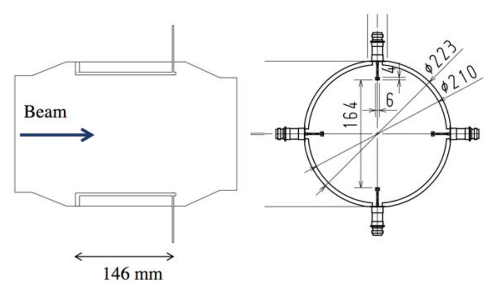

Figure 3: New BPM head with four loop-couplers.

SIGNAL PROCESSING

Signal Processing Flow

Signals are transmitted through 8D coaxial cables with high foamed polyethylene isolation to the oscilloscopes [7], DSO 6014 (8 bit, 1GSPS) for the original BPMs and DSO-X 4034A (8 bit, 2.5GSPS, thinning with a ratio of 1/3) for new BPMs.

Raw signals from the BPMs include fluctuations and noises in high frequencies (Fig. 4). We apply bandpass digital filter of the following coefficients:

$$y_n = b_0 x_n + b_2 x_{n-2} - a_1 y_{n-1} - a_2 y_{n-2} \quad (1)$$

† takeshi.toyama@kek.jp

ISBN: 978-3-95450-184-7 doi:10.18429/JACoW-IPAC2018-WEPAL020

$$b_0 = 0.1, b_2 = -0.1, a_1 = -1.970, a_2 = 0.9704$$

The frequency spectrum of the original signal (black) and the frequency spectrum of the filter (red) are shown in Fig. 5. The pass-band peak is matched to the second harmonic of the RF frequency, ~3.4 MHz. Filtered signals are shown in Fig. 6. The fluctuations are filtered out. Then peak-to-peak values are taken as the final BPM output signals, V_1, V_2, V_3, V_4.

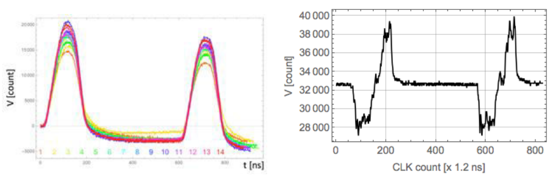

Figure 4: Signals of original and new BPMs. Colors shown in the bottom indicate the BPM#.

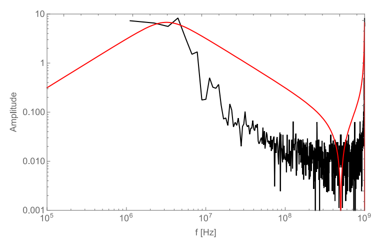

Figure 5: Frequency spectra of the BPM signal (black line) and the band pass filter (red line).

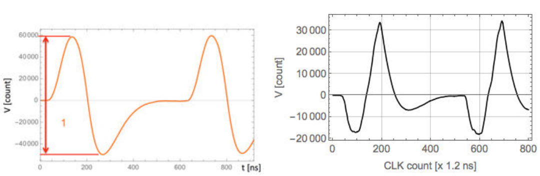

Figure 6: Filtered BPM signals.

Conversion from Four Electrode Signals to the Moments

The relation between the BPM outputs, and the multipole moments can be expressed as [8],

$$\begin{bmatrix} \hat{V}_1 \\ \hat{V}_2 \\ \hat{V}_3 \\ \hat{V}_4 \end{bmatrix} = \begin{bmatrix} C_{10} & C_{1x} & C_{1y} & C_{1q} & C_{1Q} & C_{1s}\cdots \\ C_{20} & C_{2x} & C_{2y} & C_{2q} & C_{2Q} & C_{2s}\cdots \\ C_{30} & C_{3x} & C_{3y} & C_{3q} & C_{3Q} & C_{3s}\cdots \\ C_{40} & C_{4x} & C_{4y} & C_{4q} & C_{4Q} & C_{4s}\cdots \end{bmatrix} \begin{bmatrix} 1 \\ \langle x \rangle \\ \langle y \rangle \\ \langle x^2 - y^2 \rangle \\ \langle 2xy \rangle \\ \langle x^3 - 3xy^2 \rangle \\ \vdots \end{bmatrix}$$

by generalizing the expression of induced charge on the electrode surface of opening angle, Δθ, due to a line charge at (x, y),

$$\sigma(r,\phi,R,\theta_n) = \frac{\lambda(r,\phi)\Delta\theta}{2\pi}\left[1 + 2\frac{x}{R}cos\theta_n + 2\frac{y}{R}sin\theta_n + 2\frac{x^2-y^2}{R^2}cos2\theta_n + \frac{4xy}{R^2}cos2\theta_n + 2\frac{x^3-3xy^2}{R^3}cos3\theta_n \cdots\right].$$

Here $\hat{V}_1, \hat{V}_2, \hat{V}_3, \hat{V}_4$ are normalized voltages divided by $\Sigma = V_1 + V_2 + V_3 + V_4$. Taking up to normal quadrupole mode, we obtain

$$\begin{matrix} 1 \\ <x> \\ <y> \\ <x^2 \quad y^2> \end{matrix} = \begin{matrix} c_{11} & c_{12} & c_{13} & c_{14} \\ c_{21} & c_{22} & c_{23} & c_{24} \\ c_{31} & c_{32} & c_{33} & c_{34} \\ c_{41} & c_{42} & c_{43} & c_{44} \end{matrix} \quad \begin{matrix} \hat{V}_1 \\ \hat{V}_2 \\ \hat{V}_3 \\ \hat{V}_4 \end{matrix} \tag{2}$$

The matrix elements are evaluated with the boundary element method. For the original BPMs

Inner diameter	0.23 m	0.20 m
$c_{11} = c_{12} = c_{13} = c_{14}$	1	1
$c_{21} = -c_{22} = c_{33} = -c_{34}$	0.124	0.108
$c_{41} = -c_{42} = c_{43} = -c_{44}$	0.00873	0.00668

the other elements are all zero.

For the new BPMs

Inner diameter	0.21 m
$c_{11} = c_{12} = c_{13} = c_{14}$	1
$c_{21} = -c_{22} = c_{33} = -c_{34}$	0.0983
$c_{41} = -c_{42} = c_{43} = -c_{44}$	0.00494

the other elements are all zero.

Finally, we get from $\langle x \rangle$, $\langle y \rangle$ and $q = \langle x^2 - y^2 \rangle$,

$$\sigma_x^2 - \sigma_y^2 = q - \langle x \rangle^2 + \langle y \rangle^2.$$

The dipole moment as a function of a beam position of line charge are depicted in Fig. 7. The blue line is a BEM result and the red line is a linear approximation corresponding to the coefficients, c_{21}, c_{22}, c_{33} and c_{34}.

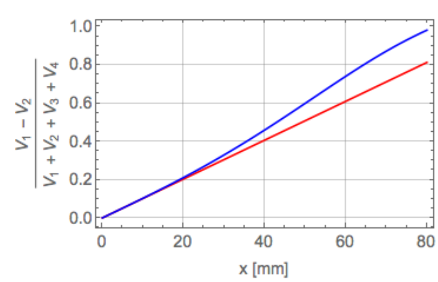

Figure 7: Dipole moment response of the BPM.

The quadrupole moments as a function of x^2-y^2 of line charge are depicted in Fig. 8. The blue line is a BEM result and the red line is a linear approximation corresponding to the coefficients, c_{41}, c_{42}, c_{43} and c_{44}.

ISBN: 978-3-95450-184-7 doi:10.18429/JACoW-IPAC2018-WEPAL020

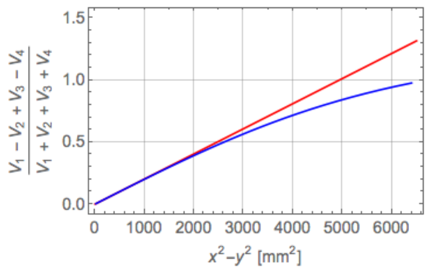

Figure 8: Quadrupole moment response of the BPM.

FIT OF EMITTANCES WITH THE 3-50BT OPTICS PARAMETERS

As the assumption of constant $\varepsilon_x, \varepsilon_y$ and $\sigma_{\Delta p/p}$ along the beam line seems reasonable for our case, we adopt the model below,

$$\sigma_x^2[i] - \sigma_y^2[i] = \beta_x[i] \cdot \varepsilon_x + \beta_y[i] \cdot \varepsilon_y + (\eta_x[i]^2 - \eta_y[i]^2)\sigma_{\Delta p/p}^2 \quad (3)$$

Beta and dispersion functions are given by the beam commissioning group (Fig. 9) [9]. $\varepsilon_x, \varepsilon_y, \sigma_{\Delta p/p}$ are obtained by fitting to Eq. (3). The result using the data in Jul. 4, 2017 is depicted by blue bots in Fig. 10 with the fitted value by green line. We obtain $\varepsilon_x \sim 2.5\ \pi$ mm·mmrad (σ), $\varepsilon_y \sim 3.6\ \pi$ mm·mmrad (σ), $\sigma_{\Delta p/p} \sim 0.15$ %.

Recent measurement result in Apr. 24, 2018 shows large discrepancy as depicted in Fig. 11. The currents of beam line magnets have been kept the same as before. The possible candidate is the variation at the beamline entrance.

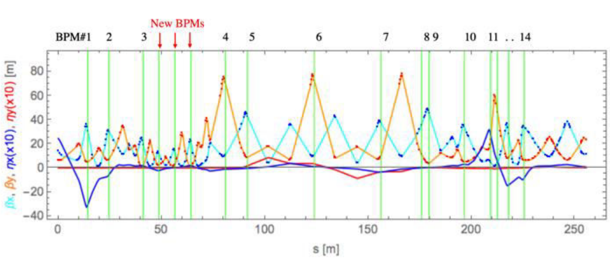

Figure 9: Lattice parameters of the 3-50BT.

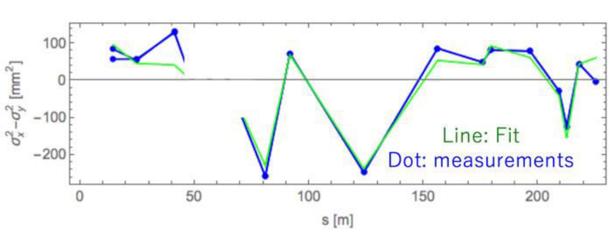

Figure 10: The measured (in Jul. 4, 2017) and fitted $\sigma_x^2 - \sigma_y^2$. Bad connector connection was corrected. Here new BPMs at s = 50 – 70 m are missing.

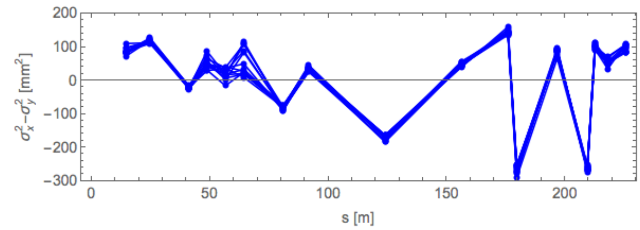

Figure 11: The measured $\sigma_x^2 - \sigma_y^2$ in Apr. 24, 2018. The magnet settings are kept same as before.

Preliminary error estimation was done in [10]. In case of |r| < 10 mm, $|x^2 - y^2| < 500$ mm^2, the systematic errors due to high order truncation are |Δx|, |Δy| < 40 µm, |Δq| < 5 mm^2. The statistical error due to noises is estimated as |Δq| < 10 mm^2.

CONCLUSION

Making full use of the BPMs data in the 3-50BT, we obtain $\sigma_x^2 - \sigma_y^2$, then reduce $\varepsilon_x, \varepsilon_y$ and $\sigma_{\Delta p/p}$ by fitting. Using the last year data the fit agrees very well with the measurement. But the recent data shows large discrepancy. Fitting including the Twiss parameters at the entrance is foreseen to understand this discrepancy. This analysis ignores the systematic error such as unbalance due to cable attenuation, mismatch etc. These errors should be corrected by beam-based-calibration.

REFERENCES

[1] M. Tejima *et al.*, "Shot-by-shot beam position monitor system for beam transport line from RCS to MR in J-PARC", Proc. of IPAC'10, 2010, p.978.

[2] M. Tejima *et al.*, "Improvement of Measurement Accuracy of the Beam Position Monitor at 3-50 BT J-PARC", Proc. of the 10th Symposium on Accelerator Science and Technology, Nagoya, Japan, August 3-5, 2013, p.1053 (*Japanese*).

[3] R. H. Miller *et al.*, "Nonintercepting Emittance Monitor", *12th Int. Conf. on High Energy Accelerators, Batavia* (1983) 602-605.

[4] T. Suwada *et al.*, "Nondestructive beam energy-spread monitor using multi-strip-line electrodes", *Phys. Rev. ST Accel. Beams* vol.6, 032801 (2003).

[5] A. Jansson, "Noninvasive single-bunch matching and emittance monitor", Phys. Rev. ST Accel. Beams vol.5, 072803 (2002).

[6] K. Satou *et al.*, "The new BPMs for the J-PARC 350BT Optics Measurements at High Radiation Fields", Proc. of the 11th Symposium on Accelerator Science and Technology, Aomori, Japan, August 9-11, 2014, p.713 (*Japanese*).

[7] http://www.keysight.com

[8] T. Toyama *et al.*, "Measurement of Transverse Multipole Moments of the Proton Beam in the J-PARC MR", proc. of IPAC2017, 2017, p.274.

[9] S. Igarashi, "3-50BT SAD (Strategic Accelerator Design) file", Mar. 2017.

[10] T. Toyama *et al.*, "Beam Size Measurement with the BPMs in the J-PARC 3-50BT", Proc. of the 14th Symposium on Accelerator Science and Technology, Sapporo, Japan, August 1-3, 2017, p.1094 (*Japanese*).